

Enhanced superconductivity in the high pressure phase of SnAs studied from first principles

P. V. Sreenivasa Reddy¹, V. Kanchana^{1,*}, T. E. Millichamp², G. Vaitheeswaran³ and S. B. Dugdale².

¹*Department of Physics, Indian Institute of Technology Hyderabad, Kandi - 502 285, Sangareddy, Telangana, India.*

²*H. H. Wills Physics Laboratory, University of Bristol, Tyndall Avenue, Bristol BS8 1TL, UK.*

³*Advanced Centre of Research in High Energy Materials (ACRHEM), University of Hyderabad, Prof. C. R. Rao Road, Gachibowli, Hyderabad - 500 046, Telangana, India.*

*Corresponding author: kanchana@iith.ac.in

Abstract

First principles calculations are performed using density functional theory and density functional perturbation theory for SnAs. Total energy calculations show the first order phase transition from an NaCl structure to a CsCl one at around 37 GPa, which is also confirmed from enthalpy calculations and agrees well with experimental work. Calculations of the phonon structure and hence the electron-phonon coupling, λ_{ep} , and superconducting transition temperature, T_c , across the phase diagram are performed. These calculations give an ambient pressure T_c , in the NaCl structure, of 3.08 K, in good agreement with experiment whilst at the transition pressure, in the CsCl structure, a drastically increased value of $T_c = 12.2 K$ is found. Calculations also show a dramatic increase in the electronic density of states at this pressure. The lowest energy acoustic phonon branch in each structure also demonstrates some softening effects. Electronic structure calculations of the Fermi surface in both phases are presented for the first time as well as further calculations of the generalised susceptibility with the inclusion of matrix elements. These calculations indicate that the softening is not derived from Fermi surface nesting and it is concluded to be due to a wavevector-dependent enhancement of the electron-phonon coupling.

Keywords: Superconductivity, Phase transition, Fermi surface, Generalised susceptibility

1. Introduction

The effect that pressure has on materials can be classified into two categories: changes to the lattice and changes to the electronic structure. One way to interpret the link between the changing of the lattice and the electronic structure is that the decrease in the interatomic distance leads to overlapping of outer electronic orbitals which will further lead to increase in the energy band widths. These subtle changes in electronic structure can lead to changes in material properties[1, 2] such as the closing of gaps in the electronic energy spectrum leading to metal-insulator transitions[3], shifts of the electronic bands leading to interband electron transitions[4, 5] or changes in the Fermi surface topology leading to Lifshitz transitions[6, 7]. Further to this, physical properties such as the electronic specific heat, superconducting transition temperature and magnetic behaviours may also change under pressure, open-

ing the door to being able to tune and hence understand specific material properties through the application of pressure.

In many 11-type compounds, pressure leads to a phase change from NaCl-type to CsCl-type structure. For instance, in the lanthanide monophosphides LnP ($Ln=La, Ce, Pr, Nd, Sm, Gd, Tb, Tm$ and Yb), the phase change occurs at pressures around 25-50 GPa[8]. In the case of the calcium chalcogenides, CaS, CaSe and CaTe, it is observed at 40 GPa, 38 GPa and 33 GPa, respectively[9]. A similar transition is also observed in IIIB-nitrides (ScN, YN) and IIIA-nitrides (GaN, InN)[10]. In the case of AgBr, an intermediate KOH-type structure is also observed from 8 to 35 GPa[11] between the NaCl-type and CsCl-type structures. The semiconducting family of tin based monochalcogenides, $SnCh$ ($Ch=O, S, Se, Te$), have band gaps ranging between 1.1 and 2.9 eV and lone pair

effects in these compounds have been studied by Lefebvre *et al.*[12]. In 1984, Losev *et al.*[13, 14] used x-ray diffraction to observe the same NaCl to CsCl structure transformation in SnAs at a pressure of around 32 GPa with an associated volume discontinuity of around 5%. Recently, superconductivity was reported in NaCl-type SnAs by Wang *et al.*[15] with a superconducting critical temperature, T_c , of 3.58 K and electron-phonon coupling constant, λ_{ep} , of around 0.62. Calculations, using density functional theory (DFT) and density functional perturbation theory (DFPT), have also been performed by Tütüncü *et al.*[16] on NaCl-type SnAs to investigate the electronic structure and hence the electron-phonon coupling, finding good agreement with experimental work. Further DFT calculations by Shrivastava *et al.*[17] have looked at the effect of pressure on the electronic structure of SnAs, further demonstrating the structural change that occurs. Recently Hase *et al.*[18] reported that the moderate charge fluctuation and electron phonon interaction is the cause for superconductivity at ambient pressure.

Pressure has long been known to have a profound effect on the superconducting properties of elements and compounds[19, 20]. Recent studies achieved a world record in high superconducting transition temperature with a value of 203 K at the pressure of 200 GPa by Drozdov *et al.*[21] in H₂S highlighting the importance of pressure in the investigation of superconductors. In SnO, Forthaus *et al.*[22] observed the appearance of a superconducting phase under pressure which is having dome like shape with a maximum T_c value 1.43 K at around 9.3 GPa and also found the disappearance of superconductivity above the pressure of 16 GPa. As well as inducing superconductivity, pressure can have the effect of enhancing T_c , motivating the investigation of the effect that pressure has on the superconducting properties of SnAs, a structurally similar system to SnO, but one that is *already* superconducting at ambient pressure.

In this work, DFPT has been employed to investigate the important changes in phonon structure and superconducting properties that occur when simulating the effect of pressure in SnAs across the phase change between the NaCl and CsCl-type structures. Furthermore, using DFT, calculations of the generalised susceptibility of SnAs are performed to ascertain the role of the electronic structure in the softening of certain phonon modes. In section 2, the details of the computational methods are discussed. In section 3, the results of these calculations are presented, including the vibrational spectra of SnAs in both structures as well as the superconducting properties across the phase change. The Fermi surface of SnAs is also presented for the first

time as well as a numerical analysis of its role in the phonon softening. Conclusions are given in section 4.

2. Computational details

The planewave pseudopotential formalism of DFT implemented within the QUANTUM ESPRESSO [23] code has been used for structural and volume optimization of the present compound. This same code was used to compute the phonon dispersions and electron-phonon interactions using DFPT. The local density approximation (LDA) to the exchange correlation functional was used for all calculations and the electron-ion interaction is described using norm-conserving pseudopotentials. The maximum planewave cut-off energy is 120 Ry and the electronic charge density is expanded up to 480 Ry. A $16 \times 16 \times 16$ k-point grid within the Brillouin zone (BZ) is used for the phonon calculations. Gaussian broadening of 0.005 Ry and a $8 \times 8 \times 8$ uniform grid of q -points is used for the calculation of the phonons.

Density functional calculations have been performed in the present work to calculate the band structure, density of states and Fermi surface. The Full-Potential Linearized Augmented Plane Wave (FP-LAPW) method as implemented in WIEN2k [24] code is used. We have used local density approximation (LDA)[25] for the exchange correlation potential. Throughout the calculations, the R_{MT} (radius of muffin tin spheres) value for each atom was fixed as 2.2 *a.u.*, 2.4 *a.u.* for As and Sn atoms respectively. For the energy convergence, the criterion $R_{MT} * K_{max} = 7$ was used, where K_{max} is the plane wave cut-off. The potential and charge density were Fourier expanded up to $G_{max} = 12 \text{ a.u.}^{-1}$. All electronic structure calculations are performed with $44 \times 44 \times 44$ grid of k points in the Monkhorst-Pack[26] scheme which gives 2168 and 2300 k -points for NaCl and CsCl-types respectively in the irreducible part of the Brillouin Zone (BZ). Tetrahedron method [27] was used to integrate the Brillouin zone. Energy convergence up to 10^{-5} Ry is used to get proper convergence of the self consistent calculation. Birch-Murnaghan [28] equation of state was used to fit the total energies as a function of primitive cell volume to obtain the bulk modulus. We have checked the effect of spin-orbit coupling (SOC) and have not found any significant changes at the Fermi level with the inclusion of SOC. Further calculations are performed without including SOC.

The calculations of the real and imaginary parts of the generalised susceptibility, $\chi(\mathbf{q})$, were performed using eigenvalues and occupancies as calculated within the full-potential linear augmented planewave (FP-LAPW) framework as implemented within the ELK code [29].

Table 1: Calculated lattice parameter (a) in Å, bulk modulus (B) in GPa, total density of states ($N(E_F)$) in states/eV/f.u. and Sommerfeld coefficient (γ) in the units of $mJ/molK^2$ for SnAs at ambient condition NaCl-type and compared with experimental[15, 42] and other theoretical[16, 18] values.

Parameters	Calculated	Exp	other theory
a	5.684	5.72513[15], 5.72[42]	5.812[16]
B	75.38	-	62.1[16]
$N(E_F)$	0.63	-	0.68[16], 0.63[18]
γ	1.49	2.18[15]	1.49[18]

140 The importance of the inclusion of matrix elements
has recently been stressed [30] and the calculations of
 $\chi(\mathbf{q})$ in this work are presented both with and without
their inclusion for comparison. These matrix elements
have been calculated within the same framework as the
eigenvalues and occupancies and have been performed
145 on a k-point grid of $32 \times 32 \times 32$.

3. Results and discussions

To begin with, calculations to reproduce the structural
transition that has been seen experimentally[13, 14] and
presented in other works[17] are performed. The total
energy has been calculated as a function of relative vol-
ume for both the NaCl and CsCl forms of SnAs to find
the stable ground state as plotted in Fig. 1(a). From this
it is evident that at ambient pressure, SnAs stabilizes in
the NaCl-type cubic structure (space group $Fm\bar{3}m$ (No.
225)) with atomic positions As (0.00, 0.00, 0.00) and
Sn (0.50, 0.50, 0.50) in agreement with the recent DFT
study by Shrivastava *et al.*[17]. From the same figure
it is also observed from the crossover of the two energy
parabolaes that SnAs undergoes a phase transition
150 from NaCl-type to CsCl-type (space group $Pm\bar{3}m$ (No.
221)) at a compression of around $V/V_0=0.76$. At this
pressure, a volume collapse of around 4.34% is seen,
in good agreement with Demishev *et al.*[14]. The cal-
culated lattice parameter and bulk modulus values are
given in Table 1 for the NaCl-type structure. The cal-
culated lattice parameter is close to the experimental
value, the discrepancy being due to the inherent under-
binding that the LDA provides. For the NaCl structure,
the calculated bulk modulus value of 75.38 GPa is in
155 good agreement with the results of Tütüncü *et al.*[16].
The change in enthalpy as a function of pressure has
also been calculated to compute the exact transition
pressure, as given in Fig. 1(b), and it is observed that
the phase transition occurs at 37 GPa.

175 Calculations of the electronic structure, performed as
part of this research agree well with previous works
[15, 16, 17]. The calculated band structure along differ-

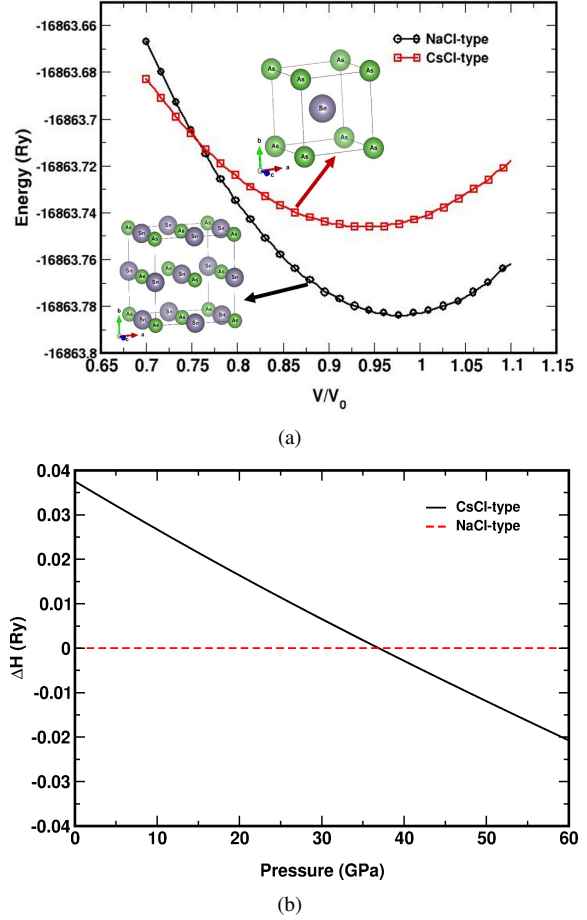


Figure 1: (a) Total energy as a function of relative volume for SnAs where circle and square symbols represent the NaCl and CsCl phases respectively. (b) Change in enthalpy against pressure to demonstrate the phase change between NaCl and CsCl type at a pressure of 37 GPa.

ent high symmetry directions is given in Fig. 2(a) at ambient condition. From the band structure, we have observed only one band to cross the Fermi level (E_F) from conduction band to valence band at Γ , X and K high symmetry points. This implies that the Fermi surface corresponding to the band might have multiple sheets. At Γ point this band has major contribution from As- p states and at L point around 1 eV it has sufficient interaction with other conduction bands leading to increased contribution from Sn- p states. The overall major contribution to this band stems from As- p states. The low lying valence band in the band structure plots at around -11 eV is due to the As- s states. The bands above this and up to E_F have major contribution from As- p , Sn- s and Sn- p states. Above E_F , the bands are due to the 'p' states of both the atoms.

To probe more at E_F , we have calculated the total and atom projected density of states (DOS) for SnAs at ambient condition and are plotted in Fig. 3(a). From the plots, it is clear that low lying peak at -11 eV is due to the As- s states as discussed in the band structure. Another peak at -8 eV is due to the 's' states of Sn atom. The total DOS at Fermi level ($N(E_F)$) is found to be 0.63 states/eV/f.u which is also in agreement with the work done by Tütüncü et. al.[16]. We find the 'p'-states of both the atoms to contribute more at E_F , with As- p states dominating more than Sn- p states. We have also observed the covalent nature between the As and Sn atoms in this compound.

Purely on an electronic basis, we can begin to get an idea of the extent of the possible electron-phonon coupling within the system in the NaCl structure by calculating the electronic linear specific coefficient or Sommerfeld coefficient, γ_{calc} , and comparing it to the experimental value, γ_{exp} . This is given in Table 1. The experimental value is higher than the calculated one as the calculation explicitly neglects many-body effects and our value agree well with the theoretical work of Hase et al.[18]. The ratio of γ_{exp} to γ_{calc} , gives an estimate of the mass renormalisation, λ , through

$$\frac{\gamma_{\text{exp}}}{\gamma_{\text{calc}}} = 1 + \lambda. \quad (1)$$

Using the experimental value by Wang et al.[15] of 2.18 mJ/molK², along with the calculated value from this work of 1.49 mJ/molK², the value of λ is found to be 0.46. If we assume the dominant renormalisation comes from the coupling between the electrons and the lattice, such that we can say $\lambda = \lambda_{\text{ep}}$, then this value can be directly compared to the value of λ_{ep} of 0.62 inferred from experiment[15]. Whilst there is reasonable agreement, it should be noted that experimental mea-

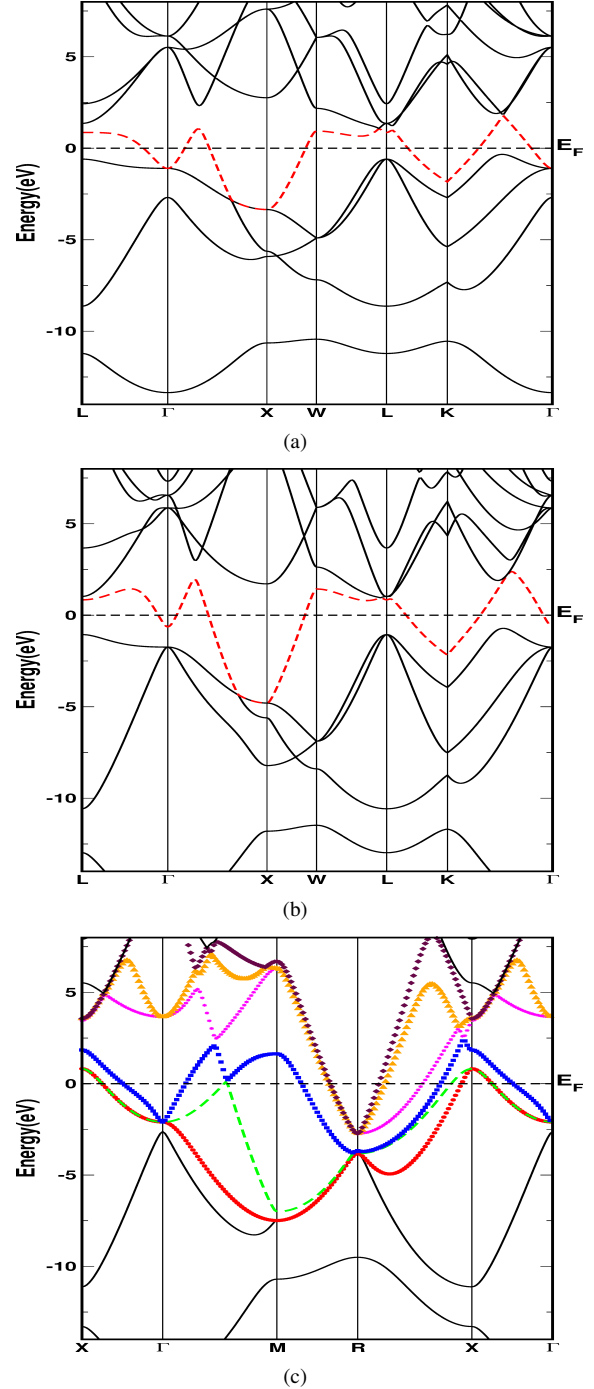


Figure 2: Band structure for SnAs (a) at ambient, (b) at transition pressure (37 GPa) for NaCl structure and (c) band structure of CsCl-type at transition pressure.

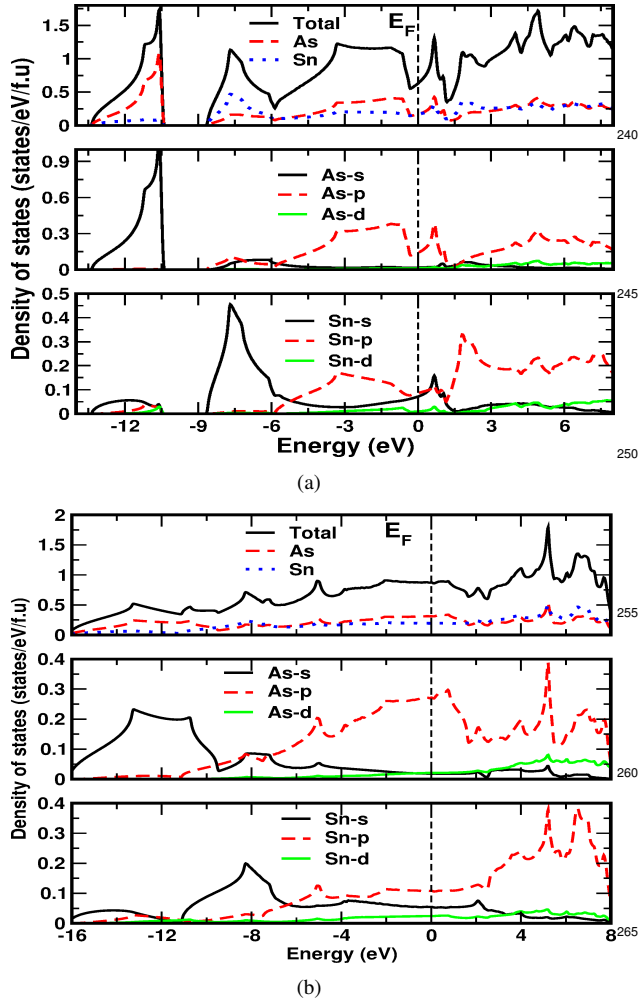


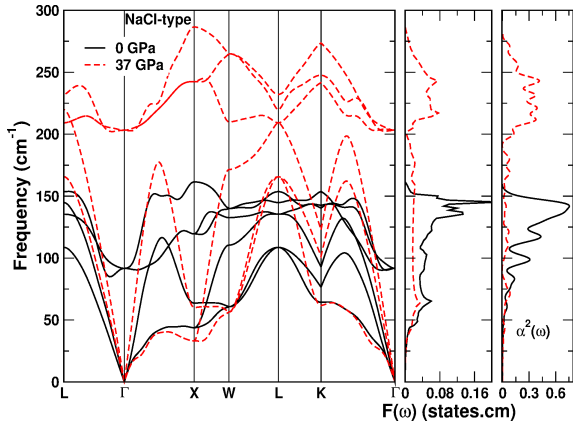
Figure 3: Total and atom projected density of states (a) at ambient NaCl-type and (b) at 37 GPa CsCl-type.

measurements of the Sommerfeld coefficient are incredibly challenging but the higher experimental value for λ_{ep} may point to the electrons coupling more strongly to special modes as has been seen previously [31, 32].

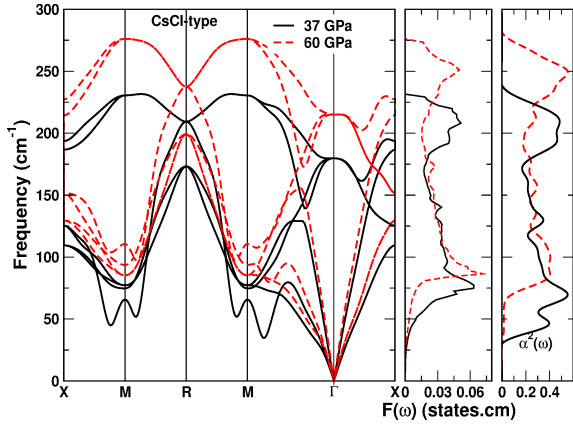
To better understand the electron-phonon coupling and how it may change on applying pressure to the system the phonon properties must first be calculated, which can be used to check the dynamical stability of the system. The phonon dispersion along different high symmetry directions is given in Fig. 4 along with the total phonon density of states (PDOS) for the NaCl structure at both ambient pressure and the transition pressure of 37 GPa (Fig. 4 (a)), and for the CsCl structure at both the transition pressure and an increased pressure of 60 GPa (Fig. 4(b)). In each case, the primitive cell has one formula unit with two atoms, leading to three acoustic and three optical branches. The absence of negative phonon frequencies indicates the dynamical stability of SnAs throughout the range of pressures.

By first looking at the total PDOS in the NaCl structure, the major peak is found near a frequency of 150 cm^{-1} and from the atom-projected phonon DOS in Fig. 4(c), it can be seen that this is derived from As. It is also observed that the higher frequency optical modes above the frequency 125 cm^{-1} are due to As and the remaining modes below 125 cm^{-1} are due to Sn. In the NaCl structure, it can be seen that the effect of the applied pressure is to raise the frequency of the majority of the branches considerably, but the broad features remain: The spectrum is dominated by As above a frequency of 200 cm^{-1} (optical modes) and the As-derived peak now sits around 225 cm^{-1} (acoustic modes), Sn remains dominant.

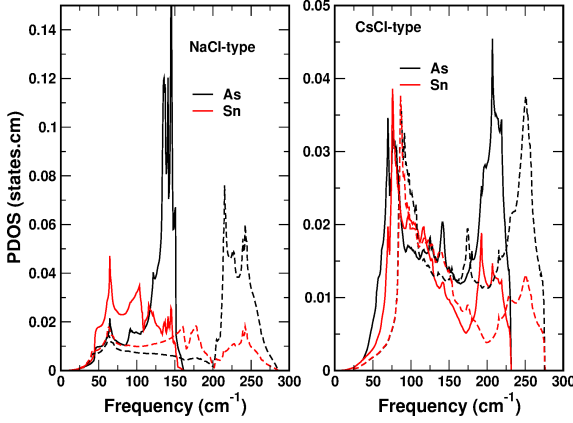
The pressure effect on superconducting properties is certainly meaningful in SnAs, as it undergoes a structural phase transition. We have calculated the band structure of NaCl-type and CsCl-type structures at transition pressure (37 GPa) and are given in Fig. 2(b) and 2(c). At 37 GPa, lattice parameter for CsCl-type is found to be 3.213 \AA . From Fig. 2(b), widening of valence band region is observed in NaCl-type together with the band shifting at Γ point. As pressure increases from 0 to 37 GPa the band at Γ point is shifted towards the E_F , resulting in decrease of As- p character with pressure. Due to this, the occupied area of the band which cross the E_F at Γ point is decreased which might have an effect on the size of electron pocket at the same Γ point in the FS. In NaCl-type, we have one single band to cross the E_F but in CsCl-type we have multiple bands to cross E_F , which is observed from Fig. 2(c). Calculated electronic density of states at 37 GPa in CsCl-type is given in Fig. 3(b), where we observed an increase in



(a)



(b)



(c)

Figure 4: (a) Phonon dispersion along with total phonon density of states and Eliashberg function for SnAs in NaCl phase at ambient and 37 GPa, (b) Phonon dispersion along with total phonon density of states and Eliashberg function for SnAs in CsCl phase at 37 and 60 GPa, (c) Atom projected phonon density of states for NaCl phase at ambient (solid lines) and 37 GPa (dotted lines) and CsCl phase at 37 (solid lines) and 60 GPa (dotted lines).

the total and partial DOS values compared with NaCl-type at E_F . As pressure increases in NaCl-type, contribution of As- p states at E_F decreases and Sn- p states increases. At 37 GPa in NaCl-type structure contribution of Sn- p states is found to be more at E_F compared to As- p states.

On transitioning into the CsCl structure (Fig. 4(b)), the frequencies of the optical modes that were increased on application of 37 GPa of pressure in the NaCl structure now reduce somewhat in energy. The spectrum now becomes more evenly distributed over energy such that the optical peak in the PDOS that now lies at 200 cm^{-1} is no longer dominant (but remains As-derived). The dominant peak in the spectrum has now shifted to the acoustic modes around 70 cm^{-1} which contain equal contributions from both As and Sn. As the pressure increases up to 60 GPa there is a hardening in the frequencies of all modes in the CsCl structure but few other alterations.

There are some interesting features to the dispersions that alter both between the two structures and with the application of pressure. In the NaCl structure, there is a degeneracy in the LA2 mode along $L-\Gamma-X$ that is broken in other directions but remains unbroken along this direction through the application of pressure. A similar degeneracy is seen in the CsCl structure along the $\Gamma-X$ direction that remains with increasing pressure. An interaction of the higher frequency acoustic modes with the optical modes is seen at various points in the BZ for both structures. In the NaCl structure, pressure acts to lift this interaction quite considerably, pulling apart the acoustic and optical modes whilst in the CsCl structure the application of further pressure has little effect on the interplay between the acoustic and optical branches.

A further interesting feature of the dispersions is the hint of softening to the lowest acoustic branch along the $\Gamma-X$ and $\Gamma-K$ directions when pressure is applied to the NaCl structure (Fig. 4(a)) as well as a much more obvious softening in the lowest acoustic branch along the $\Gamma-M$ direction and along further directions surrounding the M point in the CsCl structure that actually diminishes a little with increasing pressure. Such anomalies have been known to have significant effects on the physical properties of materials. In some of the Heusler compounds such as Ni_2MnGa [33, 34], Ni_2MnIn [35], Ni_2MnX ($X = \text{Sn, Sb}$) [36], Ni_2VAl and Ni_2NbX ($X = \text{Al, Ga, Sn}$) [37], which all have a face-centred-cubic structure like SnAs, the softening of the acoustic mode is a Kohn anomaly due to interaction of the conduction electrons with the lattice.

The mechanism behind a Kohn anomaly is one of electronic screening [38]. Under the action of a perturbation (in this case, a phonon), the electrons at the

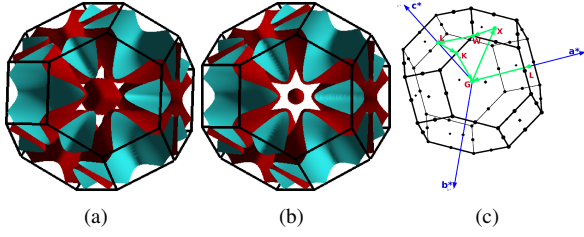


Figure 5: Fermi surface for SnAs (a) at ambient pressure, (b) at the transition pressure (37 GPa) and (c) the Brillouin zone with high symmetry points for the NaCl structure.

Fermi surface (which have access to unoccupied states) will attempt to screen it [39]. The ions of the lattice will then interact via this screened potential which modifies the phonon frequencies. The extent of this softening can therefore be dictated by how responsive the electrons are to the initial perturbation. Kohn summarised that the shape of the Fermi surface would play a vital role in this mechanism [38]. To investigate whether the softening seen here in SnAs is also a signature of a Kohn anomaly, the results of both Fermi surface and generalised susceptibility calculations are presented.

The calculated Fermi surface (FS) at ambient pressure in the NaCl structure is given in Fig. 5(a). The electron pocket at Γ point seems to possess parallel sheets along $\Gamma - X$ direction (the direction of the observed softening in this structure) indicating a possible nesting feature in this direction. On application of pressure the Fermi surface changes slightly, see Fig. 5(b), and this Γ -centred electron pocket becomes smaller. The Fermi surface of the CsCl structure at the transition pressure is given in Fig. 6, demonstrating six bands crossing the Fermi level, E_F . In terms of nesting features, the third sheet (seen in Fig. 6(c)), due to band 15, contains parallel sections that could lead to an electronic instability.

Such a visual inspection of the nesting features of a Fermi surface, however, is not sufficient, as was shown by Johannes *et al.*[40]. Through calculating both the real and imaginary parts of the generalised susceptibility, $\chi(\mathbf{q})$, where \mathbf{q} is the wavevector of the perturbation, an assessment can be made as to the geometrical nesting properties of the Fermi surface (in the imaginary part($\chi''(\mathbf{q})$)) as well as the response that the electrons will have (through the real part($\chi'(\mathbf{q})$)). A true nesting effect will be seen through singularities in both the real *and* imaginary parts at the same wavevector, showing the electronic response at a particular \mathbf{q} (possibly corresponding to the wavevector of the observed softening) is a consequence of the geometry of the Fermi surface.

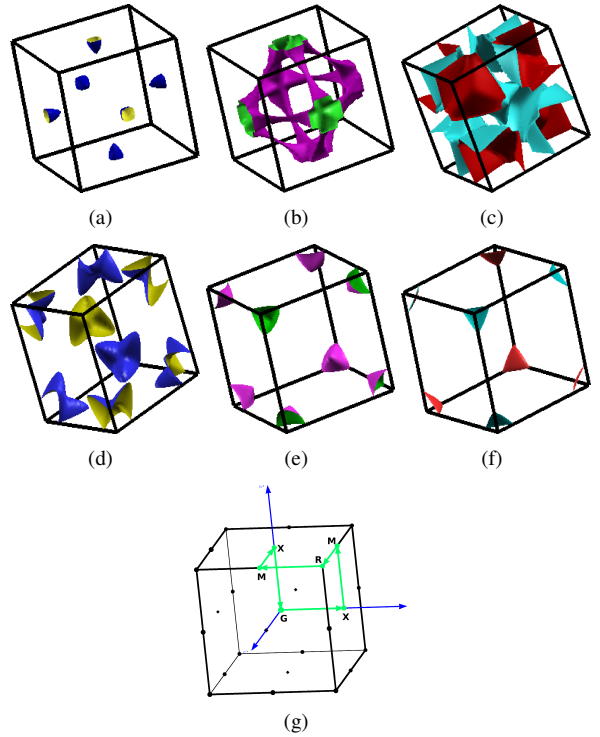


Figure 6: Fermi surface for SnAs in the CsCl structure at the transition pressure of 37 GPa for (a) band no. 13, (b) band no. 14, (c) band no. 15, (d) band no. 16, (e) band no. 17, (f) band no. 18 and (g) the Brillouin zone for the CsCl structure.

370 $\chi(\mathbf{q})$ has been calculated in both the NaCl and CsCl
 structures and is shown in Fig. 7. In the NaCl structure,
 a peak is seen in both the real and imaginary parts
 at a wavevector of $[0.0, 0.0, 0.1] \times 2\pi/a$, when using
 the constant matrix element approximation (CMA), in-
 375 dicated a strong electronic response that is driven by
 the shape of the Fermi surface. However, if the ma-
 trix elements are included in the calculation of the real
 part($\chi'(\mathbf{q})$), as is done in Fig. 7(b), the peak is strongly
 suppressed to become just a shoulder. The shoulder
 380 hints that the electrons are still somewhat more co-
 ercible at this wavevector but it is by no means a strong
 enough response to drive the observed softening of the
 phonons. Equally, when looking at the CsCl structure,
 a similar story emerges. Along the [111] direction in
 Fig. 7(c) there is a broad peak in both the real and
 385 imaginary parts of $\chi(\mathbf{q})$ when using the CMA around
 $[0.33, 0.33, 0.33] \times 2\pi/a$, in the region in which we see
 the strong softening of the phonons of SnAs in the CsCl
 structure. Once again, though, with the inclusion of ma-
 390 trix elements (Fig. 7(d)), the feature is strongly sup-
 pressed such that the electronic system would not be ca-
 pable of producing the softening seen along that direc-
 tion. With Fermi surface nesting unable to explain the
 observed softening, this points towards a \mathbf{q} -dependent
 395 enhancement of the electron-phonon coupling.

Having determined the phonon structure, the
 electron-phonon coupling can be calculated to explore
 the effect of pressure on the superconducting properties.
 This Eliashberg function, $\alpha^2F(\omega)$, (the phonon density
 400 of states weighted by both the phonon linewidth and
 the electronic DOS) gives us the energy-dependent cou-
 pling of the electrons to the phonons. $\alpha^2F(\omega)$ can be
 represented as shown below.

$$\alpha^2F(\omega) = \frac{1}{2\pi N(\epsilon_f)} \sum_{qj} \frac{v_{qj}}{\hbar\omega_{qj}} \delta(\omega - \omega_{qj}) \quad (2)$$

405 This function is related to the phonon DOS ($F(\omega) =$
 $\sum_{qj} \delta(\omega - \omega_{qj})$) and differs from the phonon DOS by
 having a weight factor $1/2\pi N(\epsilon_f)$ inside the summation.
 In the above formula $N(\epsilon_f)$ is the electronic density of
 states at the E_F and v_{qj} is the phonon line width which
 410 can be represented as below.

$$v_{qj} = 2\pi\omega_{qj} \sum_{kmn} |g_{(k+q)m, kn}^{qj}|^2 \delta(\epsilon_{kn} - \epsilon_F) \delta(\epsilon_{(k+q)m} - \epsilon_F) \quad (3)$$

where Dirac delta function express the energy conser-
 vation conditions and g is the electron phonon ma-
 trix element. From the Eliashberg function, a total
 415 electron-phonon coupling constant, λ_{ep} can hence be

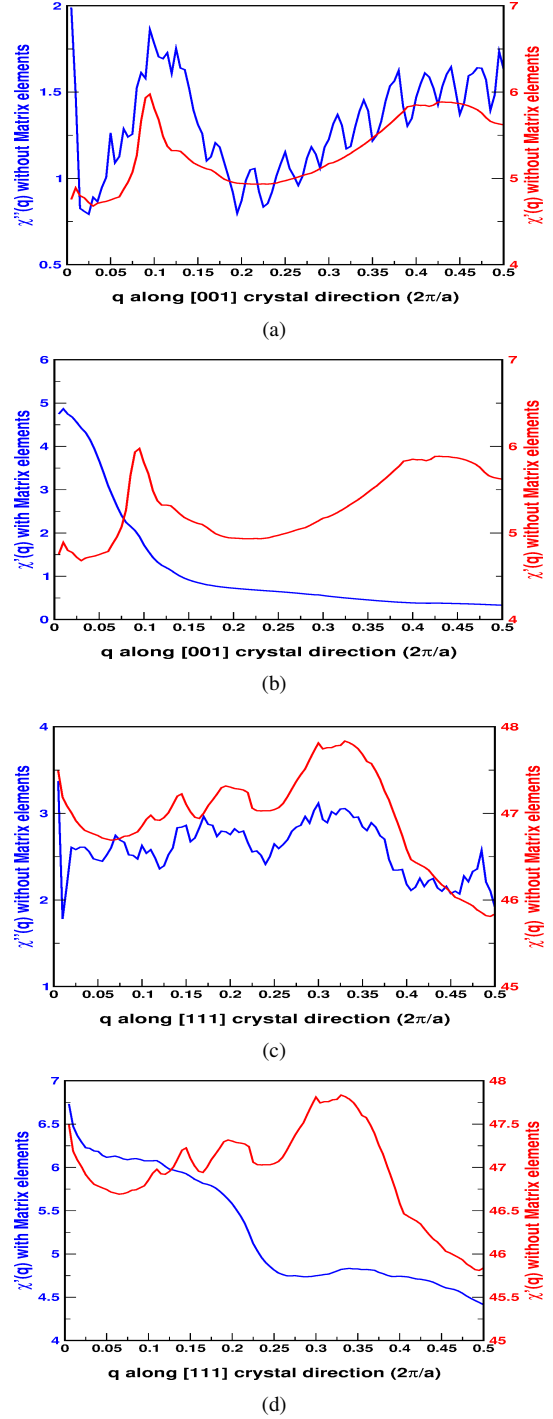


Figure 7: (a) Real($\chi'(\mathbf{q})$) and imaginary($\chi''(\mathbf{q})$) part of susceptibility without matrix elements in NaCl phase. (b) Calculated real part of susceptibility with and with out the inclusion of matrix elements for the NaCl phase. (c) Real and imaginary parts of the susceptibility without matrix elements in CsCl phase. (d) Calculated real part of susceptibility with and with out the inclusion of matrix elements for the CsCl phase.

Table 2: Superconducting properties of SnAs at ambient NaCl-type and at the transition pressure (37 GPa) CsCl-type. Experimental[15] and other theoretical[16] values are given in brackets.

Parameters	NaCl-type at 0 GPa	CsCl-type at 37 GPa
T_c (K)	3.08 (3.58[15], 3.24[16])	12.2
λ_{ep}	0.62 (0.62[15], 0.64[16])	1.08

found through

$$\lambda_{ep} = 2 \int \frac{d\omega}{\omega} \alpha^2 F(\omega). \quad (4)$$

The electron-phonon coupling constant can then be used in the Allen-Dynes formula[41] to estimate the superconducting transition temperature, T_c , through

$$T_c = \frac{\omega_{ln}}{1.2} \exp\left(-\frac{1.04(1 + \lambda_{ep})}{\lambda_{ep} - \mu^*(1 + 0.62\lambda_{ep})}\right), \quad (5)$$

where ω_{ln} is logarithmically averaged phonon frequency and μ^* is Coulomb pseudopotential. In these calculations a μ^* of 0.13 is used (values between 0.1 and 0.15 are deemed acceptable).

The calculated Eliashberg functions for the NaCl and CsCl structures are shown in Fig. 4(a) and (b), whilst the total electron phonon-coupling constants and associated T_c values are given in Table 2. Furthermore Fig. 8 demonstrates the evolution of λ_{ep} , T_c and ω_{ln} with increasing pressure, across the structural phase transition. In the case of NaCl under ambient pressure, in Fig. 4(a), the Eliashberg function indicates that there is stronger coupling to the optical phonon modes and this coupling decreases across the entire range of frequencies when the NaCl structure is put under 37 GPa of pressure. This will also be manifest in the total electron phonon coupling constant which, from Fig. 8, initially decreases as the pressure is increased before flattening towards the transition pressure. This has the effect of also decreasing T_c to essentially zero prior to the structural transition. The ambient pressure values of λ_{ep} and T_c in the NaCl structure in Table 2 agree well with both experimental[15] and computational[16] studies.

At the structural transition into the CsCl structure, in Fig. 8, a remarkable increase in both λ_{ep} and hence T_c is seen. Comparing these values to those found under ambient pressure, λ_{ep} increases almost twofold to 1.08, leading to a T_c of 12.2 K, a fourfold increase. From the Eliashberg function in Fig. 4(b), it can be seen that the coupling in the CsCl structure is more broadly constant across the range of frequencies with some signs of enhancement of the coupling both in the optical region around 200 cm^{-1} and in the acoustic modes around 45 cm^{-1} and 70 cm^{-1} . Interestingly this enhancement in

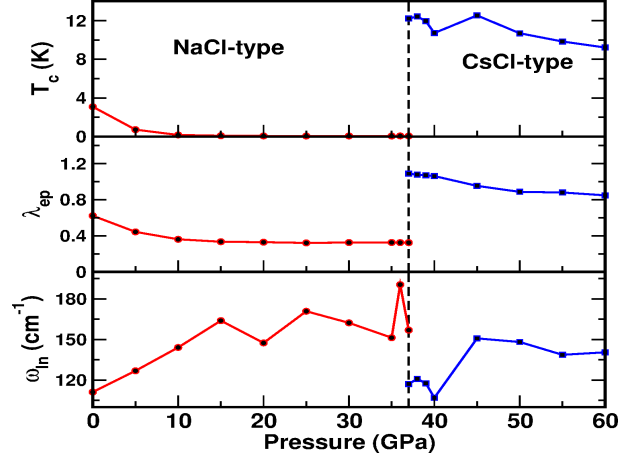


Figure 8: Pressure dependence of T_c , λ_{ep} and ω_{ln} for NaCl-type up to 37 GPa and CsCl-type above 37 GPa.

the acoustic region is around the same energies as the phonon softening is seen, further evidence to enhanced electron-phonon coupling being the possible mechanism driving the softening. With the further increase in pressure in the CsCl structure, there is little change in the magnitude of the Eliashberg function, it simply shifts to higher energies. This can also be seen in the values for λ_{ep} calculated against pressure given in Fig. 8 which remain above the ambient pressure value and lead to a robust increase in the value of T_c compared to the ambient conditions. The slight oscillation seen in the value of T_c seems to be derived from the variation in the ω_{ln} that can also be seen in Fig. 8 rather than any electronic mechanism. This abrupt increase in T_c at the structural transition pressure is likely to be driven in part by a big change in the electronic density of states at the Fermi level. Fig. 9 demonstrates that across the transition, there is an almost twofold increase in the number of electronic states at the Fermi level which would have the affect of increasing the number of electrons available to form Cooper pairs. This dramatic increase in T_c would seem to warrant further experimental exploration but provides more evidence of the importance of pressure as a tuning parameter for superconductivity.

4. Conclusions

Density functional theory and density functional perturbation theory calculations are performed for SnAs across the pressure-induced structural phase transition. The change in structure from NaCl to CsCl is observed at a pressure of 37 GPa ($V/V_0=0.76$). A striking in-

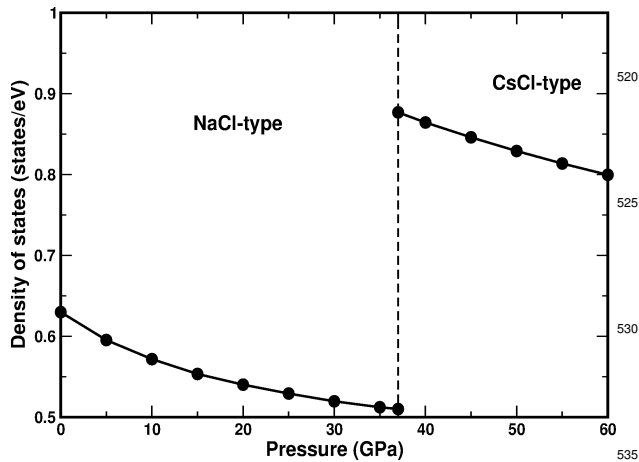


Figure 9: Total electronic density of states under pressure for SnAs in both the NaCl and CsCl structures.

crease in the total electron-phonon coupling and hence the superconducting transition temperature is seen from the ambient value of $T_c = 3.08$ K, which agrees well with experimental values, to a value in the CsCl structure at 37 GPa of $T_c = 12.2$ K. Further to this, softening of the lowest acoustic phonon mode is observed in both the NaCl and CsCl phases. Through calculations of the Fermi surface, shown for the first time, and further explorations of the generalised susceptibility with the inclusion of matrix elements, this softening is demonstrated to not derive from Fermi surface nesting. Instead, it is suggested to be from an enhanced electron-phonon coupling.

5. Acknowledgement

The authors P.V.S.R. and V.K. would like to thank the Department of Science and Technology (DST) for the financial support through SR/FTP/PS-027/2011. The authors would also like to acknowledge IIT-Hyderabad for providing the computational facility. G.V. would like to acknowledge CMSD-UoH for providing the computational facility. The authors T.E.M. and S.B.D. would like to thank the Advanced Computing Research Centre, University of Bristol (<http://www.bris.ac.uk/acrc/>) for use of their computational facilities.

- [1] J. M. Fournier and L. Manes, "Actinides-Chemistry and Physical Properties-Structure and Bonding", edited by L. Manes and Heidelberg, Springer Verlag, (1985), p. 1.
- [2] P. Ch. Sahu, N. V. Chandra Shekar, N. Subramanian, Mohammad Yousuf and K. Govindarajan "Advances in High Pressure Research in Condensed Matter", edited by S. K. Sikka, S. C. Gupta and B. K. Godwal, NISCOM, New Delhi (1997) p. 187.

- [3] A. K. McMahan, Pressure-induced changes in the electronic structure of solids, *Physica B+C* 139/140 (1986) 31-41.
- [4] H. Tups, K. Takemura and K. Syassen, Interband optical absorption and electronic $s-d$ transition in Rb and Cs at high pressures, *Phys. Rev. Lett.* 49 (1982) 1776-1779.
- [5] A. Jayaraman, "Handbook on the Physics and Chemistry of Rare Earths", edited by K. A. Gschneidner Jr and L. Eyring L, North Holland, Amsterdam, (1979) Vol 2, p. 575.
- [6] Alka B. Garg, B. K. Godwal, S. Meenakshi, P. Modak, R. S. Rao, S. K. Sikka, V. Vijay Kumar, A. Lausi and E. Bussetto, Electronic topological transition in AuX_2 ($X = In, Ga$ and Al) compounds at high pressures, *J. Phys.: Condens. Matter* 14 (2002) 10605-10608.
- [7] N. V. Chandrashekar, M. Rajagopalan, J. F. Meng, D. A. Polvani and J. V. Badding, Electronic structure and thermoelectric power of cerium compounds at high pressure, *J. Alloys Compd.* 388 (2005) 215.
- [8] Takafumi Adachi, Ichimin Shirotani, Junichi Hayashi and Osamu Shimomura, Phase transitions of lanthanide monophosphides with NaCl-type structure at high pressures, *Physics Letters A* 250 (1998) 389-393.
- [9] Huan Luo, Raymond G. Greene, Kouros Ghandehari, Ting Li and Arthur L. Ruoff, Structural phase transformations and the equations of state of calcium chalcogenides at high pressure, *Phys. Rev. B* 50 (1994) 16232-16237.
- [10] Luis Mancera, Jairo A. Rodriguez and Noboru Takeuchi, Theoretical study of the stability of wurtzite, zinc-blend, NaCl and CsCl phases in IIIb and IIIa nitrides, *Phys. Stat. Sol. (b)* 241 (2004) 2424-2428.
- [11] P. T. Jochym and K. Parlinski, Elastic properties and phase stability of AgBr under pressure, *Phys. Rev. B* 65 (2001) 024106.
- [12] I. Lefebvre, M. A. Szymanski, J. Olivier-Fourcade and J. C. Jumas, Electronic structure of tin monochalcogenides from SnO to SnTe, *Phys. Rev. B* 58 (1998) 1896-1906.
- [13] V. G. Losev, G. B. Demishev, T. I. Dyuzheva, T. N. Kolobyanina and S. S. Kabalkina, SnAs polymorphism at high-pressure to 43-GPa, *Fiz. Tverd. Tela.* 26 (1984) 3452-3454.
- [14] G. B. Demishev, S. S. Kabalkina, T. N. Kolobyanina, T. I. Dyuzheva and V. G. Losev, X-ray studies of the semiconductors SnAs, InTe, TlSe and TiSe up to 43 GPa, *High Pressure Research* 1 (1989) 325-327.
- [15] Yue Wang, Hikaru Sato, Yoshitake Toda, Shigenori Ueda, Hidenori Hiramatsu and Hideo Hosono, SnAs with the NaCl-type structure: type-I superconductivity and single valence state of Sn, *Chem. Mater.* 26 (2014) 7209-7213.
- [16] H. M. Tütüncü and G. P. Srivastava, Electron-phonon interaction and super conductivity in SnAs with the sodium chloride crystal structure, *Solid State Commun.* 221 (2015) 2427.
- [17] Deepika Shrivastava, Shweta D. Dabhi, Prafulla K. Jha and Sankar P. Sanyal, Structural phase transition, electronic and elastic properties of rocksalt structure SnAs and SnSb, *Solid State Commun.* 243 (2016) 16-22.
- [18] Izumi Hase, Kouki Yasutomi, Takashi Yanagisawa, Kousuke Odagiri and Taichiro Nishio, Electronic structure of InTe, SnAs and PbSb: Valence-skip compound or not?, *Physica C: Superconductivity and its applications* 527 (2016) 85-90.
- [19] A. V. Narlikar, "Superconductors", Oxford University Press, ISBN:9780199584116, (2014) page no. 98.
- [20] J. E. Hirsch and J. J. Hamlin, Why non-superconducting metallic elements become superconducting under high pressure, *Physica C* 470 (2010) S937-S939.
- [21] A. P. Drozdov, M. I. Erements, I. A. Troyan, V. Ksenofontov, S. I. Shylin, Conventional superconductivity at 203 kelvin at high pressures in the sulfur hydride system, *Nature* 525

- (2015) 73-76.
- 585 [22] M. K. Forthaus, K. Sengupta, O. Heyer, N. E. Christensen, A. Svane, K. Syassen, D. I. Khomskii, T. Lorenz and M. M. Abd-Elmeguid, Superconductivity in SnO: A nonmagnetic analog to Fe-based superconductors?, Phys. Rev. Lett. 105 (2010) 157001. 650
- 590 [23] P. Giannozzi, S. Baroni, N. Bonini, M. Calandra, R. Car, C. Cavazzoni, D. Ceresoli, G. L. Chiarotti, M. Cococcioni, I. Dabo, A. D. Corso, S. de Gironcoli, S. Fabris, G. Fratesi, R. Gebauer, U. Gerstmann, C. Gougoussis, A. Kokalj, M. Lazzeri, L. Martin-Samos, N. Marzari, F. Mauri, R. Maz- zarello, S. Paolini, A. Pasquarello, L. Paulatto, C. Sbraccia, S. Scandolo, G. Sclauzero, A. P. Seitsonen, A. Smogunov, P. Umari, R. M. Wentzcovitch, Quantum espresso: a modular and open-source software project for quantum simulations of materials, J. Phys.: Cond. Matt. 21 (2009) 395502.
- 595 [24] P. Blaha, K. Schwarz, P. Sorantin and S. B. Tricky, Full-potential, linearized augmented plane wave programs for crystalline systems, Comp. Phys. Comm., 59 (1990) 399.
- 600 [25] D. M. Ceperley and B. J. Alder, Ground state of the electron gas by a stochastic method, Phys. Rev. Lett. 45 (1980) 566.
- 605 [26] Hendrik J. Monkhorst and James D. Pack, Special points for brillouin-zone integrations, Phys. Rev. B 13 (1976) 5188.
- [27] P. Blöchl, O. Jepsen and O. K. Andersen, Improved tetrahe- dron method for brillouin-zone integrations, Phys. Rev. B 49 (1994) 16223.
- [28] Francis Birch, Finite elastic strain of cubic crystals, Phys. Rev. 71 (1947) 809.
- 610 [29] J. K. Dewhurst, S. Sharma and C. Ambrosch-Draxl, ELK FP-LAPW Code; available at <http://elk.sourceforge.net>
- [30] C. Heil, H. Sormann, L. Boeri, M. Aichhorn, W. von der Lin- den, Accurate bare susceptibilities from full-potential ab initio calculations, Phys. Rev. B 90 (2014) 115143.
- 615 [31] D. Billington, Simon A. C. Nickau, Tom Farley, Jack R. Ward, Rosie F. Sperring, Thomas E. Millichamp, David Ern- sting and Stephen B. Dugdale, Electron-phonon coupling and superconducting critical temperature of the YIr₂Si₂ and LaIr₂Si₂ high-temperature polymorphs from first-principles, J. Phys. Soc. Japan 83 (2014) 044710.
- 620 [32] David Billington, David Ernsting, Thomas E. Millichamp and Stephen B. Dugdale, Electron-phonon superconductivity in BaSn₅, Phil. Mag. 95 (15) (2015) 1728-1737.
- 625 [33] Claudia Bungaro, K. M. Rabe and A. Dal Corso, First-principles study of lattice instabilities in ferromagnetic Ni₂MnGa, Phys. Rev. B 68 (2003) 134104.
- [34] T. D. Haynes, R. J. Watts, J. Laverock, Zs. Major, M. A. Alam, J. W. Taylor, J. A. Duffy, S. B. Dugdale, Positron anni- hilation study of the Fermi surface of Ni₂MnGa, New J. Phys. 14 (2012) 035020.
- [35] S. Ağduk and G. Gökoğlu, First-principles study of elastic and vibrational properties of Ni₂MnIn magnetic shape mem- ory alloys, Eur. Phys. J. B 79 (2011) 509-514.
- 635 [36] S. Ağduk and G. Gökoğlu, Ab initio lattice dynamics of Ni₂MnX (X= Sn, Sb) magnetic shape memory alloys, J. Alloy. Compd. 511 (2012) 9-13.
- [37] P. V. Sreenivasa Reddy, V. Kanchana, G. Vaitheeswaran and David J. Singh, Predicted superconductivity of Ni₂VAI and pressure dependence of superconductivity in Ni₂NbX (X= Al, Ga and Sn) and Ni₂VAI, J. Phys.: Condens. Matter. 28 (2016) 115703.
- 640 [38] W. Kohn, Image of the Fermi surface in the vibration spec- trum of a metal, Phys. Rev. Lett. 2 (1959) 393.
- 645 [39] S. B. Dugdale, Life on the edge: a beginner's guide to the Fermi surface, Phys. Scr. 91 (2016) 053009.
- [40] M. D. Johannes and I. I. Mazin, Fermi surface nesting and the origin of charge density waves in metals, Phys. Rev. B 77 (2008) 165135.
- [41] P. B. Allen and R. C. Dynes, Superconductivity at very strong coupling, J. Phys. C: Solid State Phys. 8 (1975) L158.
- [42] S. Geller and G. W. Hull Jr., Superconductivity of intermetal- lic compounds with NaCl-type and related structures, Phys. Rev. Lett. 13 (1964) 127-129.